

## **On the Pitting Corrosion Behaviour of Pure Al by Halide Ions in Neutral Sulphate Solutions and the Effect of Some Inorganic Inhibitors**

Omar Abdullah Hazzazi

*Chemistry Department, Faculty of Applied Sciences,  
Umm Al-Qura University, Makkah, Saudi Arabia*

*Abstract.* The pitting corrosion of pure Al in neutral 0.50 M Na<sub>2</sub>SO<sub>4</sub> solution in the absence and presence of NaCl, NaBr and NaI under the influence of various experimental variables, including X<sup>-</sup> ions concentration, temperature and anodic step potential ( $E_{s,a}$ ), has been studied using potentiodynamic and potentiostatic techniques, complemented with Energy Dispersive X-ray (EDX) examinations of the electrode surface. Potentiostatic measurements showed that the overall process can be described by three stages. The first stage corresponds to the nucleation and growth of a passive oxide layer. The second and the third stages involving pit nucleation and growth, respectively. Nucleation of pit takes place after an incubation time ( $t_i$ ). The rate of pit nucleation ( $t_i^{-1}$ ) increases with increasing halide concentration, temperature, and applied potential. The pit growth current density ( $j_{pit}$ ) increases linearly with  $t^{1/2}$ , indicating that the pit growth can be described in terms of an instantaneous three dimensional growth under diffusion control. The effect of Cr<sub>2</sub>O<sub>7</sub><sup>2-</sup>, CrO<sub>4</sub><sup>2-</sup>, WO<sub>4</sub><sup>2-</sup>, and MoO<sub>4</sub><sup>2-</sup> as inorganic inhibitors on the pitting corrosion inhibition of pure Al in (0.5 M Na<sub>2</sub>SO<sub>4</sub> + 0.2 M NaCl) solution has also been studied. The presence of these anions results in an increase in the incubation time, and a decrease in the pit growth current density of Al to an extent depending on the nature and the concentration of the inorganic inhibitors. The inhibition efficiency of these inhibitors decreases in the order: Cr<sub>2</sub>O<sub>7</sub><sup>2-</sup> > CrO<sub>4</sub><sup>2-</sup> > WO<sub>4</sub><sup>2-</sup> > MoO<sub>4</sub><sup>2-</sup>.

### **1. Introduction**

Pure Al and Al alloys find a wide spread spectrum of technological applications because of their particular properties such as low density, good appearance and

corrosion resistance. The breakdown of the passivating oxide films on Al and its alloys, by aggressive anions such as halides at sufficiently positive anodic potentials is frequently responsible for the failure of Al and its alloys in aqueous halide solutions, because it usually leads to severe pitting of the underlying metal. Pitting corrosion has been studied for several decades by many researchers and detailed information is available<sup>[1-12]</sup>.

Various attempts have been made to study the influence of different ions in solution on the electrochemical, inhibiting or enhancing pitting corrosion of Al and its alloys<sup>[13-22]</sup>. Sehgal<sup>[23,24]</sup> and others<sup>[25,26]</sup> used the foil penetration technique to study the pit growth in Al alloys in NaCl solutions in the absence and presence of dichromate ions and other oxidizing agents and showed that the foil penetration time decreased, and therefore the rate of pit growth increased with increasing applied anodic potentials. The authors reported that dichromate ions have little influence on the pit growth rate at controlled anodic potentials, even when added in large concentrations. However, dichromate ions effectively inhibited pitting at open circuit when present in very small amounts.

Recently, S.S. Abd El Rehim *et al.*<sup>[27]</sup> studied the influence of halide ions and some inorganic inhibitors on the corrosion behaviour of Al and its alloys in Na<sub>2</sub>SO<sub>4</sub> solutions by means of EIS (Electrochemical Impedance Spectroscopy) measurements at OCP. The authors reported that in the absence of halide ions, the rates of corrosion of Al samples enhance with increasing concentration, acidity, and alkalinity of Na<sub>2</sub>SO<sub>4</sub> solution. The addition of the halide ions increases the corrosion rates of the Al samples.

The work described in this report was undertaken to apply the potentiostatic measurements to study the kinetics of pit nucleation of pure Al in quiescent deaerated neutral Na<sub>2</sub>SO<sub>4</sub> solutions by halide ions under the influence of different experimental variables. It was also the purpose of the present work to throw more light on the specific role that some inorganic inhibitors, such as dichromates, chromates, molybdates and tungstates, play on the corrosion inhibition processes occurring at the electrode-electrolyte interface. The importance of such study is rendered necessary by the wide utility of Al in different types of construction and industries.

## 2. Experimental

The working electrode employed in the present work was made of spec pure Al (99.998% purity). The investigated material was cut as cylindrical rod, welded with Cu-wire for electrical connection and mounted into glass tubes of appropriate diameter using Araldite to offer an active flat disc shaped surface of (0.25 cm<sup>2</sup>) geometric area, to contact the test solution. Prior to each experiment, the pretreatment of the working electrode was performed by mechanical

polishing (using a polishing machine model POLIMENT I, BUEHLER POLISHER) of the electrode surface with successive grades of emery papers down to 1200 grit up to a mirror finish, followed by alkali attack by immersing the electrode for 3 min in 0.01M NaOH at 30°C. The electrode was then, rinsed with acetone, distilled water, and finally dipped in the electrolytic cell.

The experiments were performed in a 100 cm<sup>3</sup> volume cell at 30°C±1, using Pt wire and a SCE as auxiliary and reference electrodes, respectively. The SCE was connected via a Luggin capillary, the tip of which was very close to the surface of the working electrode to minimize the IR drop. All potentials given in this paper are referred to this reference electrode.

The experiments were carried out in 0.50 M Na<sub>2</sub>SO<sub>4</sub> solutions in the absence and presence of different concentrations of NaCl, NaBr and NaI. Various concentrations (0.001-0.01 M) of Na<sub>2</sub>MoO<sub>4</sub>, Na<sub>2</sub>WO<sub>4</sub>, Na<sub>2</sub>CrO<sub>4</sub>, and K<sub>2</sub>Cr<sub>2</sub>O<sub>7</sub> were used as corrosion inhibitors. All solutions were freshly prepared from analytical grade chemical reagents using doubly distilled water and were used without further purification. For each run, a freshly prepared solution as well as a cleaned set of electrodes were used. Each run was carried out in deaerated stagnant solution purged with purified argon for 30 min at the required temperature (±1°C), using water thermostat. pH values of solutions were measured by using an ORION RESEARCH digital ion analyzer (Model 501).

The potentiodynamic current/potential curves were recorded by changing the electrode potential automatically from -2000 to 2000 mV with scanning rate of 1.0 mV s<sup>-1</sup>. The potentiostatic current/time transient measurements were carried out after a two step procedure, namely: the working electrode was first held at the starting potential (-2000 mV) for 60 s to attain a reproducible electro-reduced electrode surface. Then the electrode was suddenly polarized in the positive direction to a step anodic potential  $E_{s,a}$  at which the current transient was recorded. A Potentiostat / Galvanostat (EG&G model 273) and a personal computer were used. M352 corrosion software from EG&G Princeton Applied Research was used for the potentiodynamic polarization and the current/time transients measurements. Some experiments were repeated at least three times and the results were reproducible.

The composition of the passive oxide film grown on the surface of Al in (0.50 M Na<sub>2</sub>SO<sub>4</sub> + 0.04 M NaCl) solutions in the absence and presence of 0.004 M K<sub>2</sub>Cr<sub>2</sub>O<sub>7</sub>, Na<sub>2</sub>CrO<sub>4</sub>, Na<sub>2</sub>MoO<sub>4</sub> and Na<sub>2</sub>WO<sub>4</sub> was tested by EDX examinations using a Traktor TN-2000 energy dispersive spectrometer. For EDX examinations, the Al samples were submitted to the same surface treatment used in the potentiodynamic anodic polarization experiments, then immersed for 5 min in electrolytic solution at 25°C under potentiostatic regime at -1.60 V (*i.e.*, within the potential range of the passive region), and finally

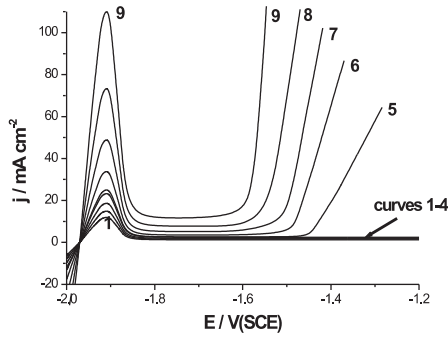
washed thoroughly and submitted to 5 min of ultrasonic cleaning in order to remove loosely adsorbed ions.

### 3. Results and Discussion

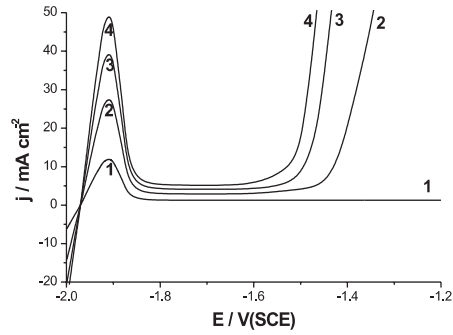
#### 3.1. Potentiodynamic Anodic Polarization Measurements

Figure 1 illustrates the potentiodynamic anodic polarization curves recorded for Al in 0.50 M Na<sub>2</sub>SO<sub>4</sub> solution (pH = 6.8) containing different concentrations (0.001-0.10 M) of NaCl between -2000 and 2000 mV (SCE) at a scan rate of 1.0 mV s<sup>-1</sup> and at 30°C. Similar results were obtained for NaBr and NaI solutions. Figure 2 represents typical potentiodynamic responses of Al in solution containing 0.50 M Na<sub>2</sub>SO<sub>4</sub> without and with 0.04 M NaX (X<sup>-</sup> = Cl<sup>-</sup>, Br<sup>-</sup>, or I<sup>-</sup>) at a scan rate of 1.0 mV s<sup>-1</sup> and at 30°C. The data reveal that the anodic span of the responses exhibits an active/passive transition. The active dissolution region involves an anodic peak (peak A) which is related to the formation of a hydrated Al<sub>2</sub>O<sub>3</sub> film on the electrode surface<sup>[28]</sup>. EDX analysis of the electrode surface within the potential range of peak A confirmed the existence of such passive film (see the details in section 3.3.). In the absence of halide ions (curve 1 in Fig. 1 and 2), the passive region extends up to 2000 mV with almost constant current density ( $j_{\text{pass}}$ ) without exhibiting a critical breakdown potential or showing any evidence of pitting attack. Similar results had been reported previously<sup>[11]</sup>. Figures 3 and 4 show, respectively, the variation of both the current density of peak A ( $j_{\text{pA}}$ ) and its potential ( $E_{\text{pA}}$ ) with  $\log C_{\text{NaX}}$  for Al in 0.50 M Na<sub>2</sub>SO<sub>4</sub> solution at 30°C. Data of Fig. 3 and 4 clearly show that the addition of the halide ions increases  $j_{\text{pA}}$  and shifts its peak potential ( $E_{\text{pA}}$ ) towards negative (active) direction, thus stimulating the active dissolution of Al in Na<sub>2</sub>SO<sub>4</sub> solution. This stimulation (*i.e.*, the peak current density and its negative potential shift) increases with increase in the concentration of the halide ions.

The present data demonstrate that the addition of Cl<sup>-</sup> ions up to a certain specific initial concentration (< 0.01 M; see curves 1-4 in Fig. 1) has practically no significant influence of the Al passivity but tends to increase  $j_{\text{pass}}$ . These findings could be attributed to general weakness and thinning of the passive film as a result of adsorption of Cl<sup>-</sup> ions on the oxide surface. The adsorbed halide ions tend to enhance the dissolution of the oxide film via the formation of soluble complexes with the Al<sup>3+</sup> ions present in the crystal lattice of the Al<sub>2</sub>O<sub>3</sub> passive film (as will be seen later). Beyond the specific concentration, the E/j curves exhibit remarkable changes in the passive region. When a certain critical potential ( $E_b$ ) is reached, the passive current density ( $j_{\text{pass}}$ ) begins to rise suddenly without any sign for oxygen evolution, indication passivity breakdown and initiation of pitting attack. Once a pit is nucleated, pitting growth is believed to proceed in the active dissolution mode. Initiation of pitting attack



**Fig. 1.** Potentiodynamic anodic polarization curves of pure Al in 0.50 M  $\text{Na}_2\text{SO}_4$  solution containing different concentrations (0.001-0.10 M) of NaCl recorded between -2000 and 2000 mV (SCE) at a scan rate of  $1.0 \text{ mV s}^{-1}$  and at  $30^\circ\text{C}$ .  
 (1) 0.001 M NaCl; (2) 0.002 M;  
 (3) 0.004 M; (4) 0.008 M; (5) 0.01 M;  
 (6) 0.02 M; (7) 0.04 M; (8) 0.08 M; (9) 0.10 M.



**Fig. 2.** Potentiodynamic anodic polarization curves of Al in 0.50 M  $\text{Na}_2\text{SO}_4$  solution without and with 0.04 M NaX ( $\text{X}^- = \text{Cl}^-$ ;  $\text{Br}^-$ , or  $\text{I}^-$ ) recorded between -2000 and 2000 mV (SCE) at a scan rate of  $1.0 \text{ mV s}^{-1}$  and at  $30^\circ\text{C}$ .  
 (1) 0.00 M NaX; (2) 0.04 M NaI;  
 (3) 0.04 M NaBr; (4) 0.04 M NaCl.

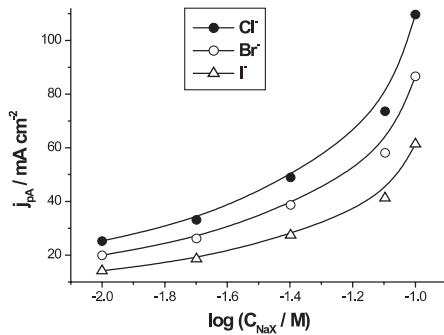


**Fig. 3.** Variation of the current density of peak A ( $j_{pA}$ ) with  $\log C_{\text{NaX}}$  for Al in 0.50 M  $\text{Na}_2\text{SO}_4$  solution at  $30^\circ\text{C}$ .

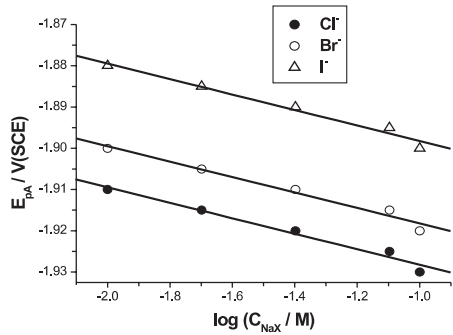
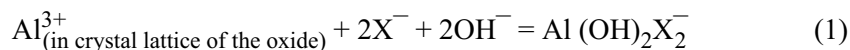


**Fig. 4.** Variation of the potential of peak A ( $E_{pA}$ ) with  $\log C_{\text{NaX}}$  for Al in 0.50 M  $\text{Na}_2\text{SO}_4$  solution at  $30^\circ\text{C}$ .

could be ascribed to adsorption of X ions on the oxide/solution interface under the influence of electric field (at the oxide/solution interface) in competition with the passive species  $\text{OH}^-$ ,  $\text{H}_2\text{O}$  dipoles and  $\text{SO}_4^{2-}$  ions for surface sites on the hydrated oxide<sup>[10,29]</sup>. The adsorption process is followed by chemical reaction between the adsorbed  $\text{X}^-$  and Al oxide cations on the hydrated oxide surface. These processes lead to the formation of  $\text{Al}(\text{OH})_2\text{X}_2^-$  complexes<sup>[30]</sup>.



The soluble complexes immediately separate from the oxide lattice and readily go in solution<sup>[31]</sup>. The process of localized dissolution of the oxide film via the formation of soluble species continues until the passive film locally dissolves. Once the passive film is locally dissolved, pit nucleates at the critical breakdown potential  $E_b$  and dissolution of the substrate metal begins. The preferential sites for halide adsorption are likely to be areas of oxide surface defects and films where the oxide thickness is smaller than in adjacent areas, and therefore the assistant electric field across the oxide/solution interface is higher<sup>[32]</sup>. The pit growth and the sudden rise in anodic current occur as a result of an increase in the  $\text{X}^-$  ion concentration, resulting from its migration and a decrease in the pH as a result of hydrolysis of  $\text{Al}^{3+}$  ions at the incipient pits.

Inspections of the data obtained display that the breakdown potential  $E_b$  depends considerably on the type and concentration of  $\text{X}^-$  ions. It is found that more positive  $E_b$  are recorded as the  $\text{Cl}^-$  ion is replaced successively by  $\text{Br}^-$  and  $\text{I}^-$  ions, indicating that the aggressiveness of the halide ions towards the stability of the passive films of Al decreases in the order:  $\text{Cl}^- > \text{Br}^- > \text{I}^-$ . These results indicate that  $\text{Cl}^-$  ion is the most aggressive anion, while  $\text{I}^-$  is the least aggressive one inspite of the fact that  $\text{Br}^-$  and  $\text{I}^-$  ions are more polarizable and hence adsorbable than  $\text{Cl}^-$  ion. The ionic radius of the halide ions seems to be an important parameter, since the ionic radii decrease in the order:  $\text{I}^- > \text{Br}^- > \text{Cl}^-$ . Therefore, it is reasonable to assume that the smaller the size of the aggressive ion, the higher is its ability to breakdown the passive layer<sup>[33]</sup>. In all cases, the  $E_b$  shifts towards more negative (active) potentials with increasing  $\text{X}^-$  ion concentration, as shown in (Fig. 5). These results agree with the data reported previously<sup>[11]</sup>.

### 3.2. Potentiostatic Current Transients

In order to gain information about the kinetics of pitting corrosion of Al by the halide ions, current densities were measured as a function of time at constant step anodic potentials  $E_{s,a}$  under different experimental conditions. Figure 6 illustrates the effect of step anodic potentials  $E_{s,a}$  (in the range between  $-1.75$  and  $-1.38$  V(SCE)) on the current vs. time transients of Al in  $0.50$  M  $\text{Na}_2\text{SO}_4$

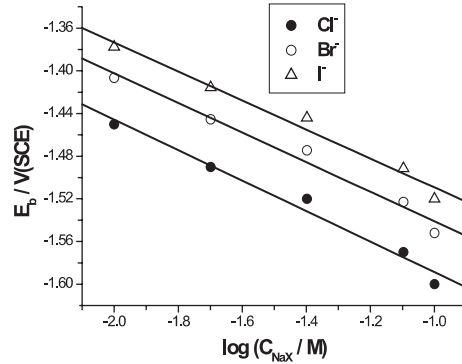


**Fig. 5.** Dependence of the breakdown potential ( $E_b$ ) on  $\log C_{NaX}$  for Al in 0.50 M  $Na_2SO_4$  solution at 30°C.

solution in the absence (Fig. 6a) and presence of 0.04 M NaCl (Fig. 6b) at 30°C. Similar results were obtained for  $Br^-$  and  $I^-$  ions. The results show that in the absence of  $Cl^-$  ions (Fig. 6a), the transient current decreases rapidly at first and then tends to attain a steady state value ( $j_{ss}$ ). The value of the steady state current density ( $j_{ss}$ ) increases with increasing  $E_{s,a}$ . The decrease in the currents are related to nucleation and growth of a hydrated oxide film on the anode surface. These data indicate that in 0.50 M  $SO_4^{2-}$  solution, aluminium can be polarized anodically without showing any evidence of pitting corrosion.

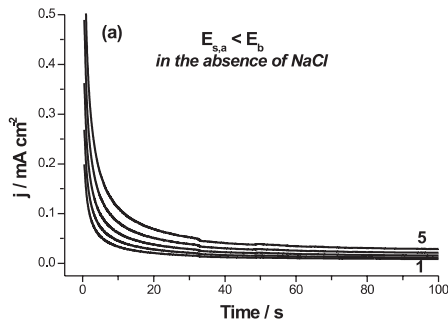


**Fig. 6(a).** Effect of step anodic potential ( $E_{s,a}$ ) on the current/time curves of Al in 0.50 M  $Na_2SO_4$  solution in the absence of NaCl at 30°C.

(1)  $E_{s,a} = -1.75$  V; (2)  $E_{s,a} = -1.70$  V; (3)  $E_{s,a} = -1.65$  V; (4)  $E_{s,a} = -1.60$  V; (5)  $E_{s,a} = -1.55$  V.

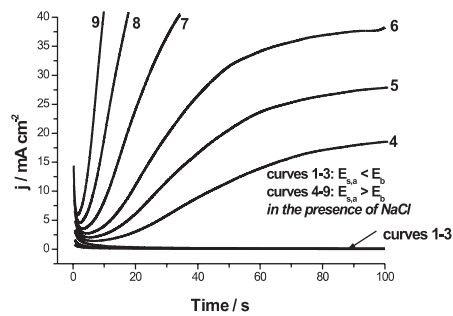


**Fig. 6(b).** Effect of step anodic potential ( $E_{s,a}$ ) on the current/time curves of Al in 0.50 M  $Na_2SO_4$  solution in the presence of 0.04 M NaCl at 30°C.

(1)  $E_{s,a} = -1.65$  V; (2)  $E_{s,a} = -1.60$  V; (3)  $E_{s,a} = -1.55$  V; (4)  $E_{s,a} = -1.48$  V; (5)  $E_{s,a} = -1.46$  V; (6)  $E_{s,a} = -1.44$  V; (7)  $E_{s,a} = -1.42$  V; (8)  $E_{s,a} = -1.40$  V; (9)  $E_{s,a} = -1.38$  V.

However, in the presence of 0.04 M  $\text{Cl}^-$  ions (Fig. 6b), the current-time curves depend on the value of  $E_{s,a}$ . For  $E_{s,a} < E_b$  (curves 1-3), the current density decreases to a steady state value, indicating that for these anodic potential steps, the  $\text{Cl}^-$  ions are not sufficient to breakdown the passive layer. In these cases, if the contribution of the double layer charging process is neglected, the overall transient current density can be related to two main processes, namely the passive layer growth ( $J_{gr}$ ) and aluminium electrodisolution through the passive layer ( $J_{dis}$ ),

$$J = J_{gr} + J_{dis} \quad (2)$$

The growth of the passive layer can be assigned to the formation of a hydrated oxide solid phase on the electrode surface. The electrodisolution of the anode through the passive layer can be explained in terms of cation diffusion from the metal/film interface to the film/solution interface. These two processes can proceed independently on the entire electrode surface. It seems that the rate of these two processes are nearly the same at the steady state current so as to keep the thickness of the passive film nearly constant.

For  $E_{s,a} > E_b$  (curves 4-9 in Fig. 6b), the transient current density initially decreases to a minimum value at a certain incubation time ( $t_i$ ), and then increases. The general trend of an increasing current suggests that pit growth is the dominant process and a number of well-developed pits could be observed following this active period. The incubation time is caused by the time required for local removal of the passive film via the sequence of  $\text{X}^-$  adsorption, penetration and formation of a readily soluble complexes. Later, pit growth, and consequently the sudden rise in the transient current density is observed. In this case, the overall transient current density is given by three contributions:

$$J = J_{gr} + J_{dis} + J_{pit} \quad (3)$$

where  $J_{pit}$  is the pit growth current density (the rising part of the current/time curves).

Further experiments were performed to clarify the influence of  $\text{X}^-$  ion concentration on the current transients of Al at 30°C and at  $E_{s,a} = -1.46$  V (this potential is more positive than  $E_b$ ); results are given in Figures 7 and 8. The effect of temperature on the current transients of Al at  $E_{s,a} = -1.46$  V was also carried out (see Fig. 9). It is found that the pit growth current density,  $J_{pit}$ , follows a current relationship with a square root of time (Fig. 10-12 are representative examples). The linear relationship suggests that the pit growth is an instantaneous three-dimensional growth under diffusion control<sup>[33]</sup>.

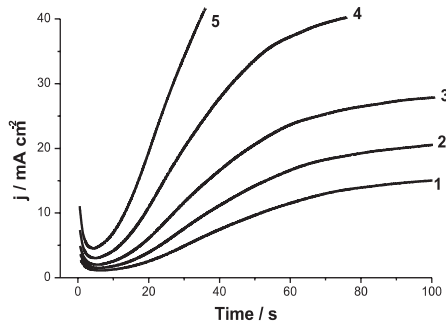


**Fig. 7.** Current/time curves recorded for Al in 0.50 M Na<sub>2</sub>SO<sub>4</sub> solution in the absence and presence of different concentrations of NaCl at 30°C and at  $E_{s,a} = -1.46$  V. (1) 0.01 M; (2) 0.02 M; (3) 0.04 M; (4) 0.08 M; (5) 0.10 M.

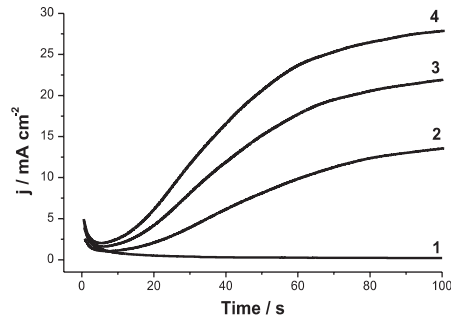


**Fig. 8.** Current/time curves recorded for Al in 0.50 M Na<sub>2</sub>SO<sub>4</sub> solution without and with 0.04 M NaX ( $X^- = Cl^-$ ,  $Br^-$ , or  $I^-$ ) at 30°C and at  $E_{s,a} = -1.46$  V. (1) 0.00 M NaX; (2) 0.04 M NaI; (3) 0.04 M NaBr; (4) 0.04 M NaCl.

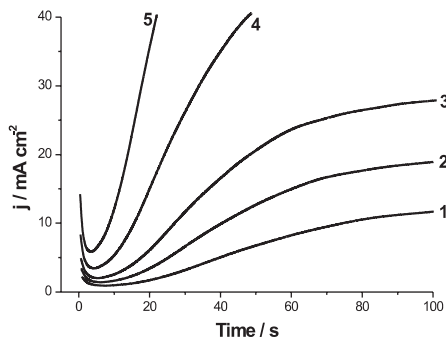


**Fig. 9.** Effect of solution temperature on the current/time curves of Al in (0.50 M Na<sub>2</sub>SO<sub>4</sub> + 0.04 M NaCl) solution at 30°C and at  $E_{s,a} = -1.46$  V. (1) 10°C; (2) 20°C; (3) 30°C; (4) 40°C; (5) 50°C.

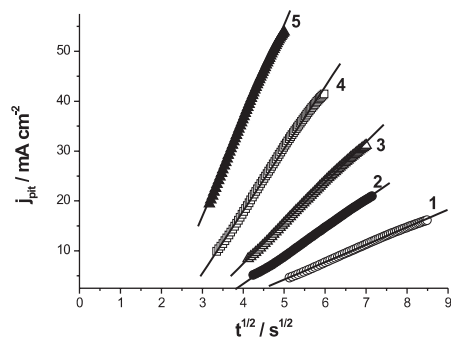


**Fig. 10.** Dependence of the pit growth current density ( $j_{pit}$ ) on  $t^{1/2}$  for pure Al in (0.50 M Na<sub>2</sub>SO<sub>4</sub> + 0.04 M NaCl) solution at 30°C and at different anodic step potentials. (1)  $E_{s,a} = -1.48$  V; (2)  $E_{s,a} = -1.46$  V; (3)  $E_{s,a} = -1.44$  V; (4)  $E_{s,a} = -1.42$  V; (5)  $E_{s,a} = -1.40$  V.

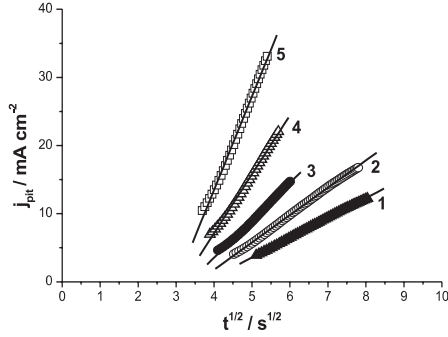


**Fig. 11.** Dependence of the pit growth current density ( $j_{\text{pit}}$ ) on  $t^{1/2}$  for pure Al in 0.50 M  $\text{Na}_2\text{SO}_4$  solution containing various concentrations of NaCl at 30°C and at  $E_{s,a} = -1.46$  V. (1) 0.01 M; (2) 0.02 M; (3) 0.04 M; (4) 0.08 M; (5) 0.10 M.

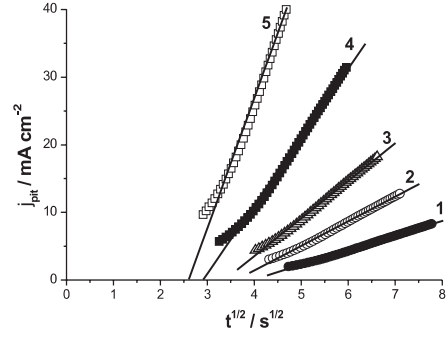


**Fig. 12.** Dependence of the pit growth current density ( $j_{\text{pit}}$ ) on solution temperature for pure Al in (0.50 M  $\text{Na}_2\text{SO}_4 + 0.04$  M NaCl) solution at  $E_{s,a} = -1.46$  V. (1) 10°C; (2) 20°C; (3) 30°C; (4) 40°C; (5) 50°C.

These results agree well with Hills model<sup>[34]</sup> which can be ascribed by the equation:

$$J_{\text{pit}} = At^{1/2} \quad (4)$$

Where  $A = 2^{3/2} z F \pi N_0 D^{3/2} C^{3/2} M^{1/2} \rho^{1/2}$ , where  $N_0$  is the number of the sites available for pitting corrosion,  $D$ ,  $C$ ,  $M$ , and  $\rho$  are the diffusion coefficient, the concentration, the molecular weight, and the density of the dissolved materials and the other terms have their usual meaning. Regarding to the data of Fig. 10-12, it can be an interception on the X-axis at zero  $J_{\text{pit}}$ , confirming that an incubation time is necessary before pit growth to occur. It is obvious that the incubation time  $t_i$  decreases (and hence the rate of pit growth increases) with increasing  $E_{s,a}$ , concentration, and temperature. These observations can be confirmed by plotting the rate of pit nucleation (*i.e.*, the number of events per unit time) defined as  $(1/t_i)$  for Al vs.  $E_{s,a}$ , concentration, and temperature, as shown in (Fig. 13-15), respectively. Figure 13 denotes that the rate of pit nucleation enhances with increasing  $E_{s,a}$ . These results agree well with the observations of Nisancioglu and Holtan<sup>[28]</sup>. The dependence of the rate of pit nucleation on  $E_{s,a}$  suggests that there is a distribution of nucleation sites of different energies which nucleate at distinct potential<sup>[35]</sup>. In other words, the more positive is the applied potential, the more will be the active sites available for pit nucleation. Moreover, an increase in  $E_{s,a}$  may increase the electric field across the passive film, and therefore enhances the adsorption of the  $X^-$  ions on

the passive electrode surface. Kolics<sup>[10]</sup> demonstrated that the adsorption of  $\text{Cl}^-$  ions on aluminium oxide surface increases with increasing anodic polarization, even above the pitting potential.

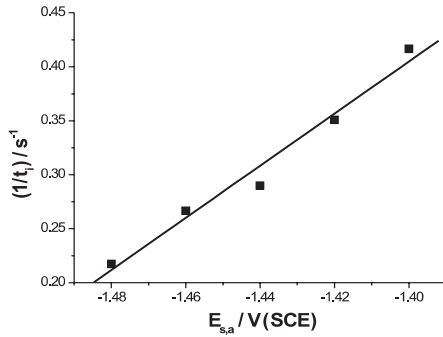


**Fig. 13.** Dependence of the rate of pit growth ( $1/t_p$ ) on  $E_{s,a}$  for pure Al in (0.50 M  $\text{Na}_2\text{SO}_4$  + 0.04 M NaCl) solution at 30°C.

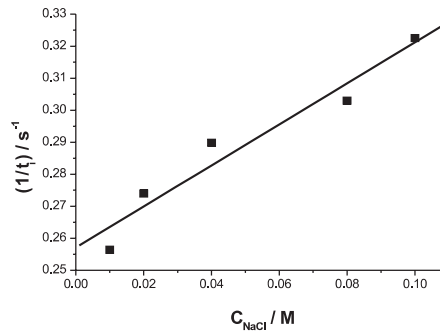


**Fig. 14.** Dependence of the rate of pit growth ( $1/t_p$ ) on  $[\text{Cl}^-]$  for pure Al in (0.50  $\text{Na}_2\text{SO}_4$  + x M NaCl) solution at 30°C and at  $E_{s,a} = -1.46$  V.

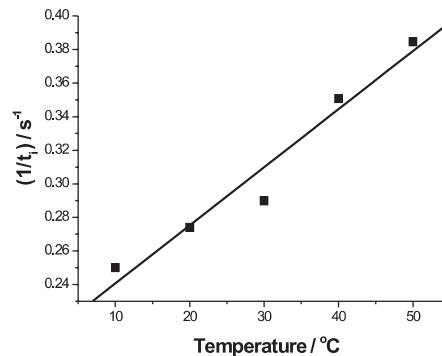


**Fig. 15.** Dependence of the rate of pit growth ( $1/t_p$ ) on solution temperature for pure Al in (0.50 M  $\text{Na}_2\text{SO}_4$  + 0.04 M NaCl) solution at  $E_{s,a} = -1.46$  V.

Figure 14 infers that, the rate of pit nucleation increases with increasing the concentration of  $\text{Cl}^-$  ions. Moreover, the results obtained showed that at a given  $\text{X}^-$  ion concentration, the rate of pit nucleation decreases in the sequence:  $\text{Cl}^- > \text{Br}^- > \text{I}^-$ , confirming the results obtained from polarization measurements, that the aggressiveness of the halide ions towards the stability of the passive films of Al decreases in the same sequence. Figure 15 shows that the rate of pit nucleation increases with increasing the temperature. The data can be interpreted on the basis of the fact that the stability and protectiveness of the passive layer of

Al decrease with increasing temperature<sup>[34]</sup>. The relation between  $\log (1/t_i)$  vs.  $T^{-1}$  for Al fits an Arrhenius-type plot (Fig. 16 is a representative example) with a slope yielding an apparent activation energies ( $E_a$ ) for pit nucleation process of about 8.82, 13.27, and 14.75 kJ mol<sup>-1</sup> for Cl<sup>-</sup>, Br<sup>-</sup>, and I<sup>-</sup>, respectively.

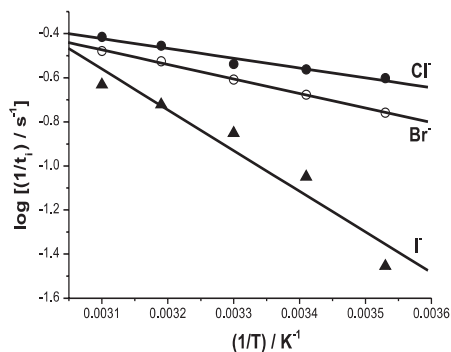


**Fig. 16.** The relation between  $\log (1/t_i)$  and  $T^{-1}$  for pure Al in 0.50 M Na<sub>2</sub>SO<sub>4</sub> solution containing 0.04 M NaX at  $E_{s,a} = -1.46$  V.

Relevant information about the pitting growth of Al can also be derived from the analysis of the rising part of the current transients which in all cases fits  $J_{\text{pit}}$  vs.  $t^{1/2}$  linear relationships. The slopes of the lines (A) can be taken as a measure of the rate of pit growth. The numerical values of A were determined and some values are listed in Tables 1-3 under various experimental conditions. It is obvious that the values of A increase with increasing  $E_s$ , [Cl<sup>-</sup>], and temperature. It follows from the data of Table 4 that the values of A for the three halide ions decrease in the sequence: Cl<sup>-</sup> > Br<sup>-</sup> > I<sup>-</sup>.

**Table 1.** Values of (A) for pure Al in 0.50 M Na<sub>2</sub>SO<sub>4</sub> solution in the absence and presence of increasing concentrations of NaX at 30°C and at  $E_{s,a} = -1.46$  V.

[X <sup>-</sup> ] / M	Slope A / (mA cm <sup>-2</sup> s <sup>-1/2</sup> )		
	Cl <sup>-</sup>	Br <sup>-</sup>	I <sup>-</sup>
0.01	0.10	0.03	0.01
0.02	0.19	0.08	0.04
0.04	0.39	0.10	0.05
0.08	0.62	0.43	0.25
0.10	1.24	0.68	0.51

**Table 2. Values of (A) for Al in (0.50 M Na<sub>2</sub>SO<sub>4</sub> + 0.04 M NaCl) solution at 30°C under the influence of increasing E<sub>s,a</sub>.**

E <sub>s,a</sub> / mV	Slope A / (mA cm <sup>-2</sup> s <sup>-1/2</sup> )
-1.48	0.15
-1.46	0.24
-1.44	0.39
-1.42	0.78
-1.40	1.38

**Table 3. Values of (A) for Al in (0.50 M Na<sub>2</sub>SO<sub>4</sub> + 0.04 M NaCl) solution at E<sub>s,a</sub> = -1.46 V under the influence of increasing temperatures.**

Temp / °C	Slope A / (mA cm <sup>-2</sup> s <sup>-1/2</sup> )
10	0.08
20	0.16
30	0.39
40	0.83
50	1.48

**Table 4. Activation energies for the initiation of pitting corrosion of Al in 0.50 M Na<sub>2</sub>SO<sub>4</sub> solution + 0.04 M NaCl solution without and with increasing concentrations of the inhibitors at 30°C and at E<sub>s,a</sub> = -1.46 V.**

	C / M			
	MoO <sub>4</sub> <sup>2-</sup>	MoO <sub>4</sub> <sup>2-</sup>	CrO <sub>4</sub> <sup>2-</sup>	Cr <sub>2</sub> O <sub>7</sub> <sup>2-</sup>
0.00	9.15	9.15	9.15	9.15
0.05	11.89	13.74	14.61	16.34
0.10	14.46	17.80	19.88	20.81
0.20	17.50	21.00	26.08	27.91
0.30	19.93	23.50	27.90	31.62
0.40	21.00	25.71	30.72	34.70

Pitting corrosion can be reduced in many instances by the presence of some inorganic anions<sup>[35]</sup>. The effects of adding different concentrations of K<sub>2</sub>Cr<sub>2</sub>O<sub>7</sub>, Na<sub>2</sub>CrO<sub>4</sub>, Na<sub>2</sub>WO<sub>4</sub> and Na<sub>2</sub>MoO<sub>4</sub> on the current/time curves of Al in solution containing 0.50 M Na<sub>2</sub>SO<sub>4</sub> and 0.20 M NaCl at different temperatures and at E<sub>s,a</sub> = -1.46 V were studied (Fig. 17 and 18 are representative examples). The data obtained show that these additives inhibit the pitting corrosion of Al, since their presence decreases both the rate of pit nucleation and the rate of pit

growth. The inhibition effect of these inhibitors decreases in the order:  $\text{Cr}_2\text{O}_7^{2-} > \text{CrO}_4^{2-} > \text{WO}_4^{2-} > \text{MoO}_4^{2-}$ . Moreover, the inhibitive effect of these inhibitors increases with increasing their concentration. Figure 19 points out the relation

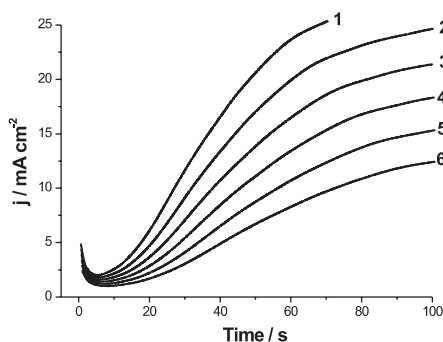


**Fig. 17.** Current transients vs. time curves recorded for pure Al in (0.50 M  $\text{Na}_2\text{SO}_4$  + 0.04 M NaCl) solution in the absence and presence of various concentrations of  $\text{WO}_4^{2-}$  at  $E_{s,a} = -1.46$  V and at  $30^\circ\text{C}$ .

(1) Blank; (2) 0.001 M; (3) 0.002 M; (4) 0.004 M; (5) 0.008 M; (6) 0.01 M.

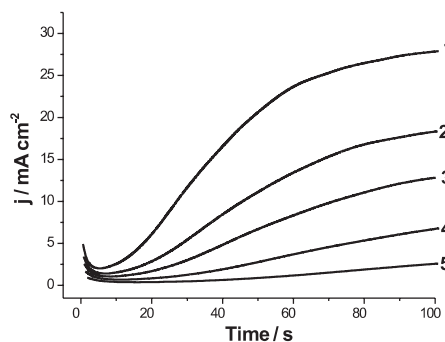


**Fig. 18.** Current transients vs. time curves recorded for pure Al in (0.50 M  $\text{Na}_2\text{SO}_4$  + 0.04 M NaCl) solution in the absence and presence of 0.004 M of the four inhibitors used at  $E_{s,a} = -1.46$  V and at  $30^\circ\text{C}$ .

(1) Blank; (2)  $\text{MoO}_4^{2-}$ ; (3)  $\text{WO}_4^{2-}$ ; (4)  $\text{CrO}_4^{2-}$ ; (5)  $\text{Cr}_2\text{O}_7^{2-}$ .

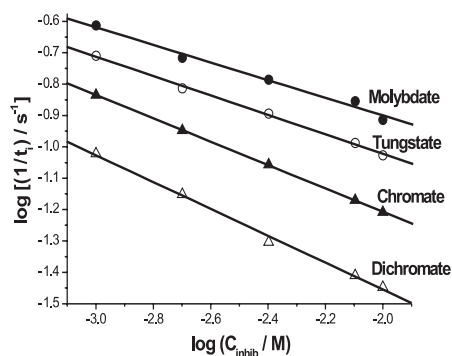


**Fig. 19.** Dependence of  $\log (l/t_i)$  on the logarithmic concentration of the inhibitors for pure Al in (0.50 M  $\text{Na}_2\text{SO}_4$  + 0.04 M NaCl) solution at  $30^\circ\text{C}$  and at  $E_{s,a} = -1.46$  V.

between  $\log (t_i^{-1})$  and  $\log [\text{inhibitor}]$ . The inhibition effect of these salts can be explained on the basis of competitive adsorption between the inorganic anions and the aggressive  $\text{Cl}^-$  ions on the passive electrode surface<sup>[36]</sup>. The adsorbed inhibitor anions impede the adsorption of  $\text{Cl}^-$  ions. Accordingly, the adsorbed inhibitor anions reduce the surface coverage of  $\text{Cl}^-$  ions and also lower the number of defect sites in the film into which the  $\text{Cl}^-$  ions can preferentially adsorb, therefore increasing pitting corrosion resistance. The inhibition effect of

the cited inorganic anions could be further explained by the involvement of these anions in the redox reactions occurring at the electrode surface. The anions  $\text{Cr}_2\text{O}_7^{2-}$ ,  $\text{CrO}_4^{2-}$ ,  $\text{WO}_4^{2-}$  and  $\text{MoO}_4^{2-}$  may undergo reduction during film formation<sup>[35,37]</sup>, resulting in the formation of  $\text{CrO}_2$ ,  $\text{WO}_2$  and  $\text{MoO}_2$ . These oxide products become part of the passivating oxide, and tend to plug its pores and defect sites, therefore imparting it better protective properties. The surface improvement undoubtedly depends on the oxidizing power of the inhibitor<sup>[23]</sup>.

The inhibition effect of these anions decreases with increasing temperature. The relation between  $\log(1/t_i)$  vs.  $T^{-1}$  fits Arrhenius-type plot (Fig. 20). From these plots, the apparent activation energies ( $E_a$ ) for pit nucleation process were determined and the values of  $E_a$  are given in Table 4. It is clear that the values of  $E_a$  decrease in the order:  $\text{Cr}_2\text{O}_7^{2-} > \text{CrO}_4^{2-} > \text{WO}_4^{2-} > \text{MoO}_4^{2-}$ , supporting the suggestion that the inhibitive effect of these inorganic compounds decreases in the same sequence. The apparent activation energy for each inhibitor decreases with its concentration.

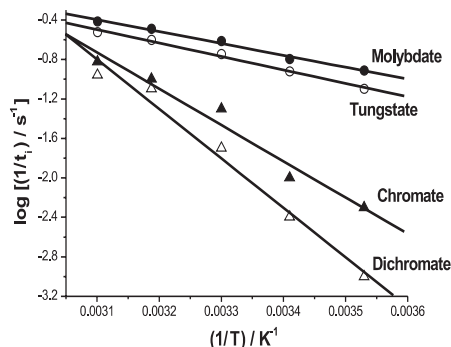
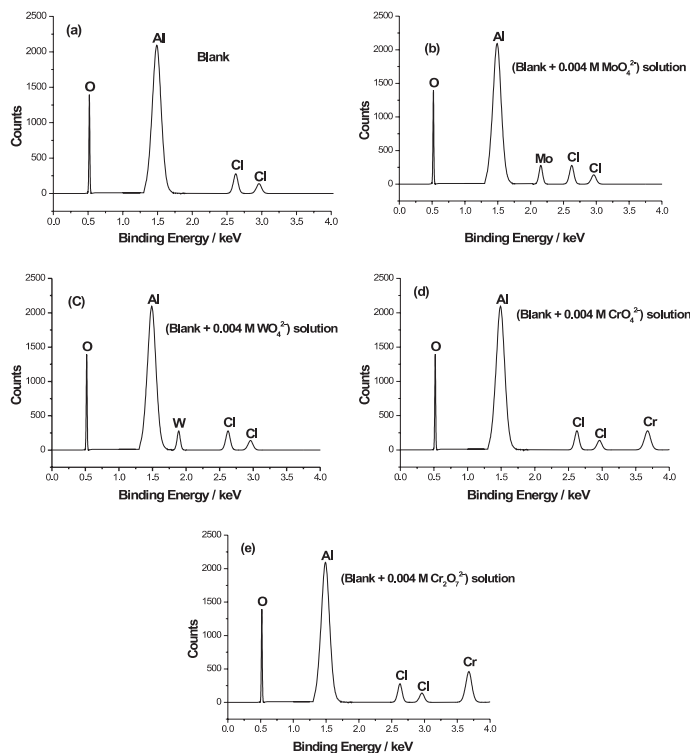


Fig. 20. The relation between  $\log(1/t_i)$  and  $T^{-1}$  for the pure Al in (0.50 M  $\text{Na}_2\text{SO}_4$  + 0.04 M  $\text{NaCl}$  + 0.004 M  $\text{inhib.}$ ) solution at  $E_{s,a} = -1.46$  V.

### 3.3. EDX Analysis of the Electrode Surface

A further insight into the processes occurring at the Al surface in (0.50 M  $\text{Na}_2\text{SO}_4$  + 0.04 M  $\text{NaCl}$ ) solution in the absence and presence of 0.004 M  $\text{Cr}_2\text{O}_7^{2-}$ ,  $\text{CrO}_4^{2-}$ ,  $\text{WO}_4^{2-}$  and  $\text{MoO}_4^{2-}$  ions was enabled by EDX data (Fig. 21). For the electrode without inhibitor treatment (Fig. 21a), Al and O signals were detected, with a ratio of about 2:3, which indicated that the passive film contained only  $\text{Al}_2\text{O}_3$ . In addition, a Cl signal was observed on the Al surface, reflecting the strong adsorption of  $\text{Cl}^-$  to the Al surface. On the other hand, the EDX spectra (Fig. 21b-e) recorded for Al in (0.50 M  $\text{Na}_2\text{SO}_4$  + 0.04 M  $\text{NaCl}$ ) solution containing 0.004 M  $\text{Cr}_2\text{O}_7^{2-}$ ,  $\text{CrO}_4^{2-}$ ,  $\text{WO}_4^{2-}$  and  $\text{MoO}_4^{2-}$  ions showed additional lines characteristic for the existence of Cr, W and Mo, respectively.

These results demonstrate that the oxide film formed in the presence of these ions contains a certain amount of incorporated Cr, W and Mo, respectively. This indicates a deep penetration of these anions into the bulk of the passive oxide film. It may be accepted as very probable that the adsorption of these anions at the oxide surface inhibits its hydration ability through decreasing the number of adsorption sites available for water molecules, and promotes a subsequent formation of surface phases like  $\text{Cr}_2\text{O}_3$ ,  $\text{MoO}_2$  and  $\text{WO}_2$ . These oxides (the reduced form of  $\text{Cr}_2\text{O}_7^{2-}$ ,  $\text{CrO}_4^{2-}$ ,  $\text{WO}_4^{2-}$  and  $\text{MoO}_4^{2-}$  ions) become part of the passive oxide film, and tend to plug its pores and flaws, thereby imparting to it better protective properties. These results clearly demonstrate that the inhibiting influence of  $\text{Cr}_2\text{O}_7^{2-}$ ,  $\text{CrO}_4^{2-}$ ,  $\text{WO}_4^{2-}$  and  $\text{MoO}_4^{2-}$  ions is due to  $\text{Cr}_2\text{O}_3$ ,  $\text{MoO}_2$  and  $\text{WO}_2$  formation in the passive oxide film.



**Fig. 21. EDX spectra recorded for Al under potentiostatic regime at  $-1.60$  V (*i.e.*, within the potential range of the passive region) and at  $30^\circ\text{C}$  in**

- (a)  $(0.50 \text{ M Na}_2\text{SO}_4 + 0.04 \text{ M NaCl})$  solution.
- (b)  $(0.50 \text{ M Na}_2\text{SO}_4 + 0.04 \text{ M NaCl})$  solution containing  $0.004 \text{ M MoO}_4^{2-}$ .
- (c)  $(0.50 \text{ M Na}_2\text{SO}_4 + 0.04 \text{ M NaCl})$  solution containing  $0.004 \text{ M WO}_4^{2-}$ .
- (d)  $(0.50 \text{ M Na}_2\text{SO}_4 + 0.04 \text{ M NaCl})$  solution containing  $0.004 \text{ M CrO}_4^{2-}$ .
- (e)  $(0.50 \text{ M Na}_2\text{SO}_4 + 0.04 \text{ M NaCl})$  solution containing  $0.004 \text{ M Cr}_2\text{O}_7^{2-}$ .

#### 4. Conclusion

The potentiodynamic polarization and potentiostatic measurements of the pitting corrosion of pure Al in deaerated neutral 0.50 M Na<sub>2</sub>SO<sub>4</sub> solution in the absence and presence of Cl<sup>-</sup>, Br<sup>-</sup> and I<sup>-</sup> ions and some inorganic inhibitors showed that:

- (i) In pure sulphate solution no pitting can be observed. Addition of the three halide ions induces pitting corrosion at specific critical pitting potentials.
- (ii) The aggressiveness of the halide ions towards the pitting corrosion of Al and its two alloys decreases in the order: Cl<sup>-</sup> > Br<sup>-</sup> > I<sup>-</sup>.
- (iii) An incubation time ( $t_i$ ) is necessary before pit nucleation and growth to occur.
- (iv) The rate of pit nucleation ( $t_i^{-1}$ ) increases with increasing halide concentration, temperature, and applied potential.
- (v) The pit growth of Al can be described in terms of an instantaneous three dimensional growth under diffusion control.
- (vi) The presence of inorganic inhibitors such as Cr<sub>2</sub>O<sub>7</sub><sup>2-</sup>, CrO<sub>4</sub><sup>2-</sup>, WO<sub>4</sub><sup>2-</sup> and MoO<sub>4</sub><sup>2-</sup> ions decreases the pitting growth current density and increases the incubation time of Al to an extent depending on their nature and concentration.
- (vii) The inhibition efficiency of these inhibitors decreases in the order: Cr<sub>2</sub>O<sub>7</sub><sup>2-</sup> > CrO<sub>4</sub><sup>2-</sup> > WO<sub>4</sub><sup>2-</sup> > MoO<sub>4</sub><sup>2-</sup>.

#### Acknowledgements

The author wishes to thank Saudi Basic Industries Corporation "SABIC" for their financial support for this project.

#### References

- [1] Videm, K., "The Electrochemistry of Uniform Corrosion and Pitting of Aluminium", Kjeller Report 62 (Kjeller, Norway: Institute for Atomenergi), (1974).
- [2] Lenderink, H.J.W., Linden, M.V.D. and DE Wit, J.H.W., *Electrochim. Acta*, **38**: 1989 (1993).
- [3] Brett, C.M.A., *Portug. Electrochim Acta*, **7**: 123 (1989).
- [4] Brett, C.M.A., *J. Appl. Electrochem.*, **20**: 1000 (1990).
- [5] Cabot, P.L., Centellas, F.A., Perez, E. and Loukili, R., *Electrochim. Acta*, **38**: 2741 (1993).
- [6] Al-Kharafi, F.M. and Badawy, W.A., *Corros.*, **54**: 377 (1998).
- [7] Kim, D. and Pyun, S., *Electrochim. Acta*, **40**: 1863 (1995).
- [8] Moshier, W.C., Davis, G.D. and Ahearn, J.S., *Corros. Sci.*, **27**: 785 (1987).
- [9] McCafferty, E., *J. Electrochem. Soc.*, **137**: 3731 (1990).
- [10] Kolics, A., Polkinghorne, J.C. and Wieckowski, A., *Electrochim. Acta*, **43**: 3605 (1998).
- [11] Bohni, H. and Uhlig, H.H., *J. Electrochem. Soc.*, **116**: 906 (1969).

- [12] **Kaesche, H.**, *Z. Physik Chem. N.F.*, **34**: 87 (1962).
- [13] **Samuels, B.W., Satoudeh, K. and Foley, R.T.**, *Corros.*, **37**: 92 (1981).
- [14] **Feres, S.E., Stefenel, M.M., Mayer, C. and Chierche, T.**, *J. Appl. Electrochem.*, **20**: 996 (1990).
- [15] **Garrigues, L., Pebere, N. and Dabosi, F.**, *Electrochim. Acta.*, **41**: 1209 (1996).
- [16] **Baumgaertner, M. and Kaesche, H.**, *Corros. Sci.*, **31**: 231 (1990).
- [17] **Carroll, W.M. and Breslin, C.B.**, *J. Br. Corros.*, **26**: 225 (1991).
- [18] **Brett, C.M.A., Gomes, I.A.R. and Martins, J.P.S.**, *Corros. Sci.*, **36**: 915 (1994).
- [19] **Zoofan, B. and Rokhlin, S. I.**, *Mater. Evaluation*, **52**: 191 (1998).
- [20] **Pride, S.T., Scully, J.R. and Hudson, J.L.**, *J. Electrochem. Soc.*, **141**: 3028 (1994).
- [21] **Zhao, J., Frankel, G.S. and McCreery, R.L.**, *Electrochem. Soc.*, **145**: 2258 (1998).
- [22] **Behrman, E.J.**, *Private Communication* (1998).
- [23] **Sehgal, A., Frankel, G.S., Zoofan, B. and Rokhlin, S.I.**, *J. Electrochem. Soc.*, **147**: 140 (2000).
- [24] **Sehgal, A., Lu, D. and Frankel, G.S.**, *J. Electrochem. Soc.*, **145**: 2834 (2000).
- [25] **Hunkeler, F. and Bohni, H.**, *Corrosion*, **37**: 645 (1981).
- [26] **Cheung, W.K., Francis, P.E. and Turnbull, A.**, *Mater. Sci. Forum*, **192-194**, Part 1, 185 (1995).
- [27] **Abdel Rehim, S.S., Hassan, H.H. and Amin, M.A.**, *J. Appl. Surf. Sci.*, **187**: 279 (2002)
- [28] **Nisancioglu, K. and Holtan, H.**, *Corros. Sci.*, **18**: 835 (1978).
- [29] **Foroulis, Z.A. and Thubrikar, M.J.**, *J. Electrochem. Soc.*, **122**: 1296 (1975).
- [30] **Foley, R.T. and Nguyen, T.H.**, *J. Electrochem. Soc.*, **129**: 464 (1982).
- [31] **Hoar, T.P.**, *Corros. Sci.*, **7**: 341 (1967).
- [32] **Richardson, J.A. and Wood, G.C.**, *Corros. Sci.*, **10**: 313 (1970).
- [33] **Refaey, S.A., Abdel Rehim, S.S., Taha, F., Saleh, M.B. and Ahmed, R.A.**, *J. Appl. Surf. Sci.*, **158**: 190 (2000).
- [34] **Nguyen, T.H. and Foley, R.T.**, *J. Electrochem. Soc.*, **126**: 1855 (1979).
- [35] **McCaffery, E., Berrett, M.K. and Murday, J.S.**, *Corros. Sci.*, **28**: 559 (1988).
- [36] **Refaey, S.A. and Abdel Rehim, S.S.**, *Electrochem. Acta.*, **42**: 667 (1966).
- [37] **Rosenfeld, I.L.**, *"Corrosion Inhibitors"*, McGraw-Hills, New York (1981).

## سلوك التآكل الثقبي للألومنيوم بواسطة أيونات الهاليدات في محاليل كبريتات الصوديوم المتعادلة ودراسة تأثير بعض المثبطات غير العضوية

عمر عبدالله هزازي

قسم الكيمياء، كلية العلوم التطبيقية، جامعة أم القرى  
مكة المكرمة - المملكة العربية السعودية

المستخلص. تم في هذا البحث دراسة التآكل الثقبي للألومنيوم في محاليل مائية متعادلة من كبريتات الصوديوم (٥٠, ٠ عياري)، في عدم وجود، وفي وجود تراكيز مختلفة من أيونات الكلوريد، والبروميد، واليوديد باستخدام الاستقطاب الأنودي البوتنشيوديناميكي، ومنحنيات التيار مع الزمن عند جهود ثابتة تحت تأثير عوامل مختلفة. وقد أوضحت نتائج منحنيات التيار مع الزمن عند جهود ثابتة، أن زمن الحضانة يقل - وبالتالي معدل التآكل الثقبي للألومنيوم يزداد - بزيادة تركيز أيونات الكلوريد، والبروميد، واليوديد، ودرجة الحرارة، والجهد الأنودي المطبق. وتم أيضاً دراسة تأثير إضافة أيونات الموليبدات، والتنجستات، والكرومات، وثنائي الكرومات على السلوك التآكلي والكهروكيميائي للألومنيوم في محلول (٥٠, ٠ عياري من كبريتات الصوديوم + ٠, ٠٤ عياري من كلوريد الصوديوم). وقد وجد أن هذه الأيونات تعمل على زيادة زمن الحضانة مما يزيد من مقاومة الألومنيوم للتآكل.